

Phase transitions and pairing signature in strongly attractive Fermi atomic gases

X. W. Guan,¹ M. T. Batchelor,^{1,2} C. Lee,³ and M. Bortz¹

¹*Department of Theoretical Physics, Research School of Physical Sciences and Engineering, Australian National University, Canberra, Australian Capital Territory 0200, Australia*

²*Mathematical Sciences Institute, Australian National University, Canberra, Australian Capital Territory 0200, Australia*

³*Nonlinear Physics Centre and ARC Centre of Excellence for Quantum-Atom Optics, Research School of Physical Sciences and Engineering, Australian National University, Canberra, Australian Capital Territory 0200, Australia*

(Received 14 May 2007; published 16 August 2007)

We investigate pairing and quantum phase transitions in the one-dimensional two-component Fermi atomic gas in an external field. The phase diagram, critical fields, magnetization, and local pairing correlation are obtained analytically via the exact thermodynamic Bethe ansatz solution. At zero temperature, bound pairs of fermions with opposite spin states form a singlet ground state when the external field $H < H_{c1}$. A completely ferromagnetic phase without pairing occurs when the external field $H > H_{c2}$. In the region $H_{c1} < H < H_{c2}$, we observe a mixed phase of matter in which paired and unpaired atoms coexist. The phase diagram is reminiscent of that of type II superconductors. For temperatures below the degenerate temperature and in the absence of an external field, the bound pairs of fermions form hard-core bosons obeying generalized exclusion statistics.

DOI: 10.1103/PhysRevB.76.085120

PACS number(s): 05.30.Fk, 03.75.Hh, 03.75.Ss, 05.30.Pr

I. INTRODUCTION

Recent achievements in manipulating quantum gases of ultracold atoms have opened up exciting possibilities for the experimental study of many-body quantum effects in low-dimensional systems.^{1–3} Experimental observation of superfluidity and phase separation in imbalanced Fermi atomic gases^{4,5} has stimulated great interest in exploring exotic quantum phases of matter with two mismatched Fermi surfaces. The pairing of fermionic atoms with mismatched Fermi surfaces may lead to a breached pairing phase⁶ and a nonzero momentum pairing phase of Fulde-Ferrell-Larkin-Ovchinnikov (FFLO) states.⁷ In general, the nature of pairing and superfluidity in strongly interacting systems is both subtle and intriguing.⁸

Pairing is well known to be a momentum space phenomenon, in which two fermions with opposite spin states form a bound pair which behaves like a boson. The bound pairs form a superfluid, while the unpaired fermions remain as a separated gas phase in momentum space. Such superfluid states with gapless excitations in ultracold atomic gases provide an exciting insight into the superfluid regime in quantum many-body physics. Fermi gases of ultracold atoms with population imbalance have been predicted to exhibit a quantum phase transition between the normal and superfluid states.^{9–12} Mismatched Fermi surfaces can appear in different quantum systems, such as type II superconductors in an external magnetic field,¹³ a mixture of two species of fermionic atoms with different densities or masses,^{9,10} and a charge neutral quark matter.^{14,15}

These exotic phases have attracted newfound interest in the one-dimensional (1D) integrable two-component Fermi gas^{16–18} which was used to study BCS–Bose-Einstein condensation crossover^{19,20} and quantum phase separation in a trapping potential.^{21,22} The 1D Fermi gases can be experimentally realized by applying strongly transverse confinement to the Fermi atomic clouds.²³ In the 1D interacting Fermi gas, the Fermi surface is reduced to the Fermi points.

The lowest excitation destroys a bound pair close to the Fermi surface. Charge and spin propagate with different velocities due to the pairwise interaction. The external magnetic field triggers energy level crossing such that the Fermi surfaces of paired fermions and unpaired fermions vary smoothly with respect to the external field. As we shall see in this paper, the presence of the external field at zero temperature has an important bearing on the nature of quantum phase transitions in 1D interacting fermions.

In general, the exact Bethe ansatz (BA) solution of any model provides reliable physics beyond mean field theory.²⁴ The thermodynamic Bethe ansatz^{18,25–29} (TBA) provides a way to obtain the ground state signature and finite temperature behavior of integrable 1D quantum many-body systems. At zero temperature, the TBA equations naturally reduce to dressed energy equations in which the external field is explicitly involved. Thus, the band fillings are subsequently varied with respect to the external field. This gives an elegant way to analyze quantum phase transitions in the presence of an external field by means of the dressed energy formalism. Our aim here is to obtain exact results from this formalism for characteristics of pairing phases and quantum phase transitions in the 1D two-component strongly attractive Fermi gas of cold atoms. We present a systematic way to obtain the critical fields and magnetic properties at zero temperature for strongly interacting fermions. We find that the bound pairs of fermions with opposite spin states form a singlet ground state when the external field $H < H_{c1}$. A completely ferromagnetic phase without pairing occurs when the external field $H > H_{c2}$. In the region $H_{c1} < H < H_{c2}$, we observe a mixed phase of matter in which paired and unpaired atoms coexist. However, in the absence of the external magnetic field, we show that the bound pairs of fermions behave like hard-core diatoms obeying nonmutual generalized exclusion statistics (GES) at temperatures much less than the binding energy.

This paper is set out as follows. In Sec. II, we present the BA solution of the 1D two-component interacting Fermi gas. The ground state properties are also analyzed. In Sec. III, we introduce the TBA in order to set up the dressed energy

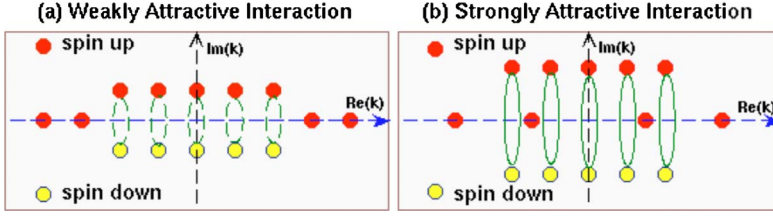


FIG. 1. (Color online) Schematic Bethe ansatz configuration of quasimomenta k in the complex plane. (a) For weakly attractive interaction, the quasimomenta of unpaired fermions sit in the outer wings of the distribution. (b) For strongly attractive interaction, they can penetrate into the central region.

formalism. The quantum phase transitions and magnetic properties are studied by means of the dressed energy formalism in Sec. IV. We discuss the distribution profiles and the thermodynamics of the 1D strongly attractive Fermi gas of atoms at low temperatures in Sec. V, along with the connection to GES. Section VI is devoted to concluding remarks.

II. MODEL

The model we consider has interacting atoms in two hyperfine levels $|1\rangle$ and $|2\rangle$, which are coherently coupled with laser or radio frequency fields. Under strong transverse confinement, the system is effectively described along the axial direction by the 1D Hamiltonian $\mathcal{H}=\mathcal{H}_0+\mathcal{H}_{int}+\mathcal{H}_c$. The first term,

$$\mathcal{H}_0 = \sum_{j=1}^2 \int \psi_j^\dagger(x) \left[-\frac{\hbar^2}{2m} \frac{d^2}{dx^2} + V(x) \right] \psi_j(x) dx, \quad (1)$$

contains the kinetic energy and the trapping potential $V(x)$. The second term,

$$\mathcal{H}_{int} = g_{1D} \int \psi_1^\dagger(x) \psi_2^\dagger(x) \psi_2(x) \psi_1(x) dx, \quad (2)$$

describes s -wave interaction and

$$\mathcal{H}_c = \frac{1}{2} \Omega \int [\psi_2^\dagger(x) \psi_1(x) + \psi_1^\dagger(x) \psi_2(x)] dx \quad (3)$$

is the coupling term. Here, $\psi_1^\dagger(x)$ and $\psi_2^\dagger(x)$ are the atomic field creation operators, g_{1D} is the 1D interaction strength, and Ω is the Rabi frequency of coupling fields.

Defining $\psi_1 = (\phi_\downarrow + \phi_\uparrow)/\sqrt{2}$ and $\psi_2 = (\phi_\downarrow - \phi_\uparrow)/\sqrt{2}$, the Hamiltonian becomes

$$\begin{aligned} \mathcal{H} = & \sum_{j=\downarrow,\uparrow} \int \phi_j^\dagger(x) \left[-\frac{\hbar^2}{2m} \frac{d^2}{dx^2} + V(x) \right] \phi_j(x) dx \\ & + g_{1D} \int \phi_\downarrow^\dagger(x) \phi_\uparrow^\dagger(x) \phi_\uparrow(x) \phi_\downarrow(x) dx \\ & - \frac{1}{2} \Omega \int [\phi_\uparrow^\dagger(x) \phi_\uparrow(x) - \phi_\downarrow^\dagger(x) \phi_\downarrow(x)] dx. \end{aligned} \quad (4)$$

The new field operators ϕ_\downarrow and ϕ_\uparrow describe the atoms in the states $|\downarrow\rangle = (|1\rangle + |2\rangle)/\sqrt{2}$ and $|\uparrow\rangle = (|1\rangle - |2\rangle)/\sqrt{2}$. This Hamiltonian also describes the 1D δ -interacting spin- $\frac{1}{2}$ Fermi gas with an external magnetic field $H=\Omega$. Here, we consider the homogeneous case $V(x)=0$ with periodic boundary condi-

tions for a line of length L .^{16,17} Unless specifically indicated, we use units of $\hbar=2m=1$. We define $c=mg_{1D}/\hbar^2$ and a dimensionless interaction strength $\gamma=c/n$ for the physical analysis, with linear density $n=N/L$, where N is the number of fermions. The intercomponent interaction can be tuned from strongly attractive ($g_{1D} \rightarrow -\infty$) to strongly repulsive ($g_{1D} \rightarrow +\infty$) via Feshbach resonances.

The model was solved by nested BA (Refs. 16 and 17) for the energy eigenspectrum

$$E = \frac{\hbar^2}{2m} \sum_{j=1}^N k_j^2 \quad (5)$$

in terms of the N BA wave numbers $\{k_j\}$, which are the quasimomenta of the fermions. They satisfy the BA equations^{16,17}

$$\begin{aligned} \exp(ik_j L) &= \prod_{\ell=1}^M \frac{k_j - \Lambda_\ell + ic/2}{k_j - \Lambda_\ell - ic/2}, \\ \prod_{\ell=1}^N \frac{\Lambda_\alpha - k_\ell + ic/2}{\Lambda_\alpha - k_\ell - ic/2} &= - \prod_{\beta=1}^M \frac{\Lambda_\alpha - \Lambda_\beta + ic}{\Lambda_\alpha - \Lambda_\beta - ic}. \end{aligned} \quad (6)$$

Here $j=1, \dots, N$ and $\alpha=1, \dots, M$, with M the number of spin-down fermions. The additional parameters $\{\Lambda_\alpha\}$ are the rapidities for the internal spin degrees of freedom.

The distribution of the quasimomenta in the complex plane was studied recently.³⁰ For weakly attractive interaction, the system describes weakly bound Cooper pairs where the quasimomenta are distributed in a BCS-like manner³⁰ [Fig. 1(a)]. In this limit, the ground state energy per unit length is given by

$$E \approx \frac{\hbar^2 n^3}{2m} \left[\frac{\gamma}{2} (1 - P^2) + \frac{\pi^2}{12} + \frac{\pi^2}{4} P^2 \right], \quad (7)$$

with the polarization $P=(N-2M)/N$. The bound state has a small binding energy $\epsilon_b = \hbar^2 n |\gamma| / m$ and is therefore unstable against thermal fluctuations. For strongly attractive interaction, the bound pairs form hard-core bosons [Fig. 1(b)]. The energy per unit length derived directly from Eq. (6) is³⁰

$$\begin{aligned} E \approx & \frac{\hbar^2 n^3}{2m} \left\{ -\frac{(1-P)\gamma^2}{4} + \frac{P^3 \pi^2}{3} \left[1 + \frac{4(1-P)}{|\gamma|} \right] \right. \\ & \left. + \frac{\pi^2 (1-P)^3}{48} \left[1 + \frac{(1-P)}{|\gamma|} + \frac{4P}{|\gamma|} \right] \right\}, \end{aligned} \quad (8)$$

with binding energy $\epsilon_b = \hbar^2 n^2 \gamma^2 / (4m)$. Generally, the total momentum for bound pairs and that for unpaired fermions are both zero. Thus, the BA roots for the model with popu-

lation imbalance do not show sufficient evidence for the existence of a FFLO state which might exist in the asymmetric BCS pairing models.^{9,12} In FFLO states, the unpaired fermions have an asymmetric distribution at the Fermi surface resulting in a net total momentum for bound pairs.⁷

III. THERMODYNAMIC BETHE ANSATZ

The TBA has been well established in quantum integrable systems.^{18,25–29} For the sake of completeness, we sketch the main idea and results of the TBA for the fermion model in this section. At zero temperature, all quasimomenta k_i of N atoms form two-body bound states, i.e., $k_j = \Lambda'_j \pm i\frac{1}{2}c$, accompanied by the real spin parameter Λ'_j . Here, $j=1, \dots, M$. However, at finite temperature, spin quasimomenta form complex strings $\Lambda_{\alpha j}^n = \Lambda_{\alpha}^n + i\frac{1}{2}(n+1-2j)c$, with $j=1, \dots, n$.¹⁸ Here, the number of strings $\alpha=1, \dots, N_n$. Λ_{α}^n is the position of the center for the length- n string on the real axis. The number of n strings N_n satisfies the relation $M = M' + \sum_n n N_n$. There are M' real Λ'_j and there are $N-2M'$ real k_i for unpaired fermions. In the presence of a magnetic field, the ground state consists of two Fermi seas: one contains bound pairs and the other contains unpaired fermions.

In the thermodynamic limit, i.e., $N, L \rightarrow \infty$ with N/L finite, it is assumed that the distributions of Bethe roots are sufficiently dense along the real axis. After introducing the root distribution functions $\sigma(k)$, $\rho(k)$, and $\xi_n(k)$ for paired fermions, unpaired fermions, and the spin n string, as well as their hole densities $\sigma^h(k)$, $\rho^h(k)$, and $\xi_n^h(k)$, the BA equations [Eq. (6)] can be transformed into the forms¹⁸

$$\begin{aligned}\sigma(k) + \sigma^h(k) &= \frac{1}{\pi} - a_2 * \sigma(k) - a_1 * \rho(k), \\ \rho(k) + \rho^h(k) &= \frac{1}{2\pi} - a_1 * \sigma(k) - \sum_{n=1}^{\infty} a_n * \xi_n(k), \\ \xi_n(\Lambda) + \xi_n^h(\Lambda) &= a_n * \rho(\Lambda) - \sum_{m=1}^{\infty} T_{nm} * \xi_m(\Lambda).\end{aligned}\quad (9)$$

Here, $*$ denotes the convolution integral $(f * g)(\lambda) = \int_{-\infty}^{\infty} f(\lambda - \lambda')g(\lambda')d\lambda'$ and

$$a_m(\lambda) = \frac{1}{2\pi} \frac{m|c|}{(mc/2)^2 + \lambda^2}.\quad (10)$$

The function $T_{nm}(\lambda)$ can be found in Takahashi's book.¹⁸

The equilibrium states at finite temperature T are described by the equilibrium quasiparticle and hole densities. The partition function $Z = \text{tr}(e^{-\mathcal{H}/T})$ is defined as

$$Z = \sum_{\sigma, \sigma^h, \rho, \rho^h, \xi_n, \xi_n^h} W e^{-E(\sigma, \sigma^h, \rho, \rho^h, \xi_n, \xi_n^h)/T},\quad (11)$$

where the densities satisfy the BA equations [Eq. (9)] and $W := W(\sigma, \sigma^h, \rho, \rho^h, \xi_n, \xi_n^h)$ is the number of states corresponding to the given densities. By introducing the combinatorial entropy $S = \ln W$, the grand partition function can be

presented as $Z = e^{-G/T}$, where the Gibbs free energy $G = E - \mu N - HM^z - TS$. Here, μ is the chemical potential. The entropy and Gibbs free energy are given in terms of the BA root distribution functions of particles and holes for bound pairs and unpaired fermions, as well as spin degrees of freedom.

The energy per unit length is defined by

$$E = \int_{-\infty}^{\infty} \left[k^2 \rho(k) + 2 \left(k^2 - \frac{c^2}{4} \right) \sigma(k) \right] dk - M^z H.\quad (12)$$

Here, H is the external magnetic field and $M^z = (N - 2M)/2L$ denotes the atomic magnetic momentum per unit length (where the Bohr magneton μ_B and the Landé factor are absorbed into the magnetic field H).

The entropy per unit length is given by¹⁸

$$\begin{aligned}S &= \int_{-\infty}^{\infty} \{ [\sigma(k) + \sigma^h(k)] \ln[\sigma(k) + \sigma^h(k)] - \sigma(k) \ln \sigma(k) \\ &\quad - \sigma^h(k) \ln \sigma^h(k) \} dk + \int_{-\infty}^{\infty} \{ [\rho(k) + \rho^h(k)] \ln[\rho(k) + \rho^h(k)] \\ &\quad - \rho(k) \ln \rho(k) - \rho^h(k) \ln \rho^h(k) \} dk \\ &\quad + \sum_{n=1}^{\infty} \int_{-\infty}^{\infty} \{ [\xi_n(\lambda) + \xi_n^h(\lambda)] \ln[\xi_n(\lambda) + \xi_n^h(\lambda)] \\ &\quad - \xi_n(\lambda) \ln \xi_n(\lambda) - \xi_n^h(\lambda) \ln \xi_n^h(\lambda) \} d\lambda.\end{aligned}\quad (13)$$

The equilibrium states are determined by the minimization condition of the Gibbs free energy, which gives rise to a set of coupled nonlinear integral equations—the TBA equations.¹⁸ In terms of the dressed energies $\epsilon^b(k) := T \ln[\sigma^h(k)/\sigma(k)]$ and $\epsilon^u(k) := T \ln[\rho^h(k)/\rho(k)]$, for paired and unpaired fermions, these are

$$\begin{aligned}\epsilon^b(k) &= 2 \left(k^2 - \mu - \frac{1}{4}c^2 \right) + Ta_2 * \ln[1 + e^{-\epsilon^b(k)/T}] \\ &\quad + Ta_1 * \ln[1 + e^{-\epsilon^u(k)/T}]\end{aligned}$$

$$\begin{aligned}\epsilon^u(k) &= k^2 - \mu - \frac{1}{2}H + Ta_1 * \ln[1 + e^{-\epsilon^b(k)/T}] \\ &\quad - T \sum_{n=1}^{\infty} a_n * \ln[1 + \eta_n^{-1}(k)]\end{aligned}$$

$$\begin{aligned}\ln \eta_n(\lambda) &= \frac{nH}{T} + a_n * \ln[1 + e^{-\epsilon^u(\lambda)/T}] \\ &\quad + \sum_{m=1}^{\infty} T_{nm} * \ln[1 + \eta_m^{-1}(\lambda)].\end{aligned}\quad (14)$$

The function $\eta_n(\lambda) := \xi_n^h(\lambda)/\xi_n(\lambda)$ is the ratio of the string densities. The Gibbs free energy per unit length is given by

$$G = -\frac{T}{\pi} \int_{-\infty}^{\infty} dk \ln[1 + e^{-\epsilon^b(k)/T}] - \frac{T}{2\pi} \int_{-\infty}^{\infty} dk \ln[1 + e^{-\epsilon^u(k)/T}]. \quad (15)$$

The TBA equations provide a clear picture of band fillings with respect to the field H and the chemical potential μ at arbitrary temperatures. However, it is a challenging problem to obtain analytic results for the thermodynamics at low temperatures from the TBA [Eq. (14)].

We focus on quantum phase transitions in the 1D strongly attractive Fermi gas at $T=0$ by analyzing the dressed energy equations

$$\begin{aligned} \epsilon^b(\Lambda) &= 2\left(\Lambda^2 - \mu - \frac{c^2}{4}\right) - \int_{-B}^B a_2(\Lambda - \Lambda') \epsilon^b(\Lambda') d\Lambda' \\ &\quad - \int_{-Q}^Q a_1(\Lambda - k) \epsilon^u(k) dk, \\ \epsilon^u(k) &= \left(k^2 - \mu - \frac{H}{2}\right) - \int_{-B}^B a_1(k - \Lambda) \epsilon^b(\Lambda) d\Lambda, \end{aligned} \quad (16)$$

which are obtained from the TBA equations [Eq. (14)] in the limit $T \rightarrow 0$. The dressed energy $\epsilon^b(\Lambda) \leq 0$ [$\epsilon^u(k) < 0$] for $|\Lambda| \leq B$ ($|k| \leq Q$) corresponds to the occupied states. The positive part of $\epsilon^b(\epsilon^u)$ corresponds to the unoccupied states. The integration boundaries B and Q characterize the Fermi surfaces for bound pairs and unpaired fermions, respectively. The Gibbs free energy per unit length at zero temperature is given by

$$G(\mu, H) = \frac{1}{\pi} \int_{-B}^B \epsilon^b(\Lambda) d\Lambda + \frac{1}{2\pi} \int_{-Q}^Q \epsilon^u(k) dk. \quad (17)$$

The magnetization $M^z = nP/2$ per unit length is determined by H , g_{1D} , and n through the relations

$$-\partial G(\mu, H)/\partial \mu = n, \quad -\partial G(\mu, H)/\partial H = M^z. \quad (18)$$

IV. QUANTUM PHASE TRANSITIONS

The ground state is antiferromagnetic, i.e., the number of the fermionic atoms with up-spin states and the number of the fermionic atoms with down-spin states are equal. In this case, the integral limit for the unpaired Fermi sea $Q=0$ and $\rho(k)=0$. For strong coupling, i.e., $L|c| \gg 1$, the dressed energy equations [Eq. (16)] reduce to the form

$$\epsilon^b(\Lambda) \approx 2\left(\Lambda^2 - \mu - \frac{c^2}{4}\right) - \frac{1}{2\pi} \int_{-B}^B \frac{2|c| \epsilon^b(\Lambda') d\Lambda'}{c^2 + (\Lambda - \Lambda')^2}. \quad (19)$$

For convenience of notation, we denote

$$p^b = -\frac{1}{\pi} \int_{-B}^B \epsilon^b(\Lambda) d\Lambda$$

$$p^u = -\frac{1}{2\pi} \int_{-Q}^Q \epsilon^u(k) dk \quad (20)$$

as the pressure for bound pairs and unpaired fermions. Substituting Eq. (19) into p^b , we have

$$\pi p^b \left(1 + \frac{2B}{\pi|c|}\right) \approx 4B \left(\mu - \frac{1}{3}B^2 + \frac{c^2}{4}\right). \quad (21)$$

Furthermore, from the Fermi points $\epsilon^b(\pm B)=0$, we have

$$B^2 \approx \mu + \frac{c^2}{4} - \frac{p^b}{2|c|}. \quad (22)$$

From relation (18), together with Eqs. (21) and (22), we obtain the pressure and the ground state energy per unit length as

$$\begin{aligned} p^b &\approx \frac{\hbar^2 \pi^2 n^3}{2m} \left(1 + \frac{3}{2|\gamma|}\right), \\ E_0 &\approx \frac{\hbar^2 n^3}{2m} \left\{ -\frac{\gamma^2}{4} + \frac{1}{48} \pi^2 \left[1 + \frac{1}{|\gamma|}\right] \right\}. \end{aligned} \quad (23)$$

For the strongly attractive 1D Fermi gas, the low-energy excitations split into collective excitations carrying charge and collective excitations carrying spin. This leads to the phenomenon of spin-charge separation. The spin excitation is gapped with a divergent spin velocity

$$v_s = \frac{n|\gamma|}{\sqrt{2}} \left(1 + \frac{2}{|\gamma|}\right). \quad (24)$$

Therefore, the spin sector cannot be described by a conformal field theory. However, the charge sector is still critical³¹ with central charge $C=1$ and the charge velocity

$$v_c = \frac{v_F}{4} \left(1 + \frac{1}{|\gamma|}\right) \quad (25)$$

for the fully paired ground state, where the bound pairs behave like hard-core bosons. In the above equation, $v_F = \hbar n \pi / 4m$. The bound pairs can be broken by a strong enough external field or thermal fluctuations. In the strong interaction limit, it was demonstrated in a recent experiment that the nature of the pairing is likely to be molecular and the mismatched Fermi surfaces do not prevent pairing but indeed quench the superfluidity.⁸ The state with polarization can be viewed as an ideal mixture of bosonic pairs and fermionic quasiparticles.

With polarization $0 < P < 1$, from Eq. (16), we obtain

$$\begin{aligned} p^b &\approx -\frac{4B}{\pi} \left(\frac{B^2}{3} - \mu - \frac{c^2}{4} + \frac{p^b}{2|c|} + \frac{2p^u}{|c|}\right), \\ p^u &\approx -\frac{Q}{\pi} \left(\frac{Q^2}{3} - \mu - \frac{H}{2} + \frac{2p^b}{|c|}\right), \end{aligned} \quad (26)$$

From the Fermi points $\epsilon^b(B)=0$ and $\epsilon^u(Q)=0$, we have

$$2\left(B^2 - \mu - \frac{c^2}{4}\right) + \frac{p^b}{|c|} + \frac{4p^u}{|c|} \approx 0,$$

$$Q^2 - \mu - \frac{H}{2} + \frac{2p^b}{|c|} \approx 0. \quad (27)$$

It follows that

$$p^b \approx \frac{8}{3\pi} \left(\mu + \frac{c^2}{4} - \frac{p^b}{2|c|} - \frac{2p^u}{|c|} \right)^{3/2},$$

$$p^u \approx \frac{2}{3\pi} \left(\mu + \frac{H}{2} - \frac{2p^b}{|c|} \right)^{3/2}. \quad (28)$$

With the help of relation (18) and by lengthy iteration, we find that the effective chemical potentials for pairs $\mu^b = \mu + \epsilon_b/2$ and unpaired fermions $\mu^u = \mu + H/2$ are given by

$$\mu^b \approx \frac{\hbar^2 n^2 \pi^2}{2m} \left\{ \frac{(1-P)^2}{16} \left[1 + \frac{4(1-P)}{3|\gamma|} + \frac{4P}{|\gamma|} \right] + \frac{4P^3}{3|\gamma|} \right\} \quad (29)$$

and

$$\mu^u \approx \frac{\hbar^2 n^2 \pi^2}{2m} \left\{ P^2 \left[1 + \frac{4(1-P)}{|\gamma|} \right] + \frac{(1-P)^3}{12|\gamma|} \right\}. \quad (30)$$

These results can give explicit chemical potentials for the two different species:

$$\mu_{\uparrow} = \mu + H/2, \quad \mu_{\downarrow} = \mu - H/2. \quad (31)$$

In addition, we have the total chemical potential $\mu = \partial E / \partial n - HP/2$. Here, the energy per unit length with polarization [Eq. (8)] follows from the relation $E = n\mu - G(\mu, H) + nHP/2$. Indeed, the energy obtained from the TBA formalism is in agreement with the result [Eq. (8)] derived from the BA.³⁰ The integration boundaries

$$B \approx \frac{n\pi(1-P)}{4} \left[1 + \frac{(1-P)}{2|\gamma|} + \frac{2P}{|\gamma|} \right],$$

$$Q \approx n\pi P \left[1 + \frac{2(1-P)}{|\gamma|} \right] \quad (32)$$

are the largest quasimomentum for bound pairs and unpaired fermions.

Analysis of the dressed energy equations [Eq. (16)] shows that the fully paired ground state with $M^z = 0$ is stable when the field $H < H_{c1}$, where

$$H_{c1} \approx \frac{\hbar^2 n^2}{2m} \left(\frac{\gamma^2}{2} - \frac{\pi^2}{8} \right). \quad (33)$$

This critical field makes the excitation gapless. If the external field $H > H_{c1}$, the *pairing gap*, defined by $\Delta = (H_{c1} - H)/2$, is completely diminished by the external field. Slightly above the critical point H_{c1} , the system has a linear field-dependent magnetization

$$M^z \approx \frac{2(H - H_{c1})}{n\pi^2} \left(1 + \frac{2}{|\gamma|} \right), \quad (34)$$

with a finite susceptibility

$$\chi \approx \frac{2}{n\pi^2} \left(1 + \frac{2}{|\gamma|} \right). \quad (35)$$

This behavior differs from the Pokrovsky-Talapov-type phase transition occurring in a gapped spin liquid. We note that this smooth phase transition in the attractive Fermi gas is reminiscent of the transition from the Meissner phase to the mixed phase in type II superconductors.¹³

On the other hand, if the external field $H > H_{c2}$, where

$$H_{c2} \approx \frac{\hbar^2 n^2}{2m} \left[\frac{\gamma^2}{2} + 2\pi^2 \left(1 - \frac{4}{3|\gamma|} \right) \right], \quad (36)$$

all bound pairs are broken and the ground state becomes a normal ferromagnetic state of fully polarized atoms. Slightly below H_{c2} , the phase transition is determined by the linear field-dependent relation

$$M^z \approx \frac{1}{2} n \left[1 - \frac{(H_{c2} - H)}{4n^2 \pi^2} \left(1 + \frac{10}{3|\gamma|} \right) \right], \quad (37)$$

with a finite susceptibility

$$\chi \approx \frac{1}{8n\pi^2} \left(1 + \frac{10}{3|\gamma|} \right). \quad (38)$$

A mixed phase occurs in the region $H_{c1} < H < H_{c2}$, with coexistence of spin singlet bound pairs and unpaired fermions with ferromagnetic order. The external field-magnetization relation

$$\frac{H}{2} \approx \frac{\hbar^2 n^2}{2m} \left\{ \frac{\gamma^2}{4} + 4\pi^2 (m^z)^2 \left[1 + \frac{4(1-2m^z)}{|\gamma|} - \frac{8m^z}{3|\gamma|} \right] - \frac{\pi^2}{16} (1-2m^z)^2 \left(1 + \frac{8m^z}{|\gamma|} \right) \right\} \quad (39)$$

follows by Eqs. (29) and (30). It indicates the energy transfer relation among the kinetic energy variation $\Delta E_k = \mu^u - \mu^b$, the binding energy ϵ_b , and the Zeeman energy $\mu_B H$:

$$\Delta E_k + \epsilon_b = \mu_B H, \quad (40)$$

which qualitatively agrees with the relation identified in experiment.²³ In the above equation, we take the Bohr magneton $\mu_B = 1$ and $m^z = M^z/n$.

Figure 2(a) shows the magnetization and the susceptibility for $|c| = 10$ and $n = 0.5, 1, 1.5, 2$. The magnetization gradually increases from $M^z = 0$ to $n/2$ as the field increases from H_{c1} to H_{c2} . It is important to note that the points of intersection at $H = \epsilon_b$ indicate where the Fermi surface of unpaired fermions exceeds the one for the bound pairs. This point separates the mismatched pairing phase into different breached pairing phases.^{6,9} The susceptibility shows discontinuities at the critical points, with $\chi = 0$ for $H < H_{c1}$ and $H > H_{c2}$. However, χ is finite and quickly decreases in the vicinity of H_{c1} . For larger densities [Fig. 2(c) illustrates the case $n = 2$], χ slowly increases as $H \rightarrow H_{c2}$. We note that the coexistence of pairing and magnetization in the 1D attractive Fermi gas is similar to the Shubnikov phase of superconductivity and magnetization in type II superconductors.¹³

Figure 3 shows the phase diagram in the n - H plane for the particular value $|c| = 10$. As $n \rightarrow 0$, the two critical fields ap-

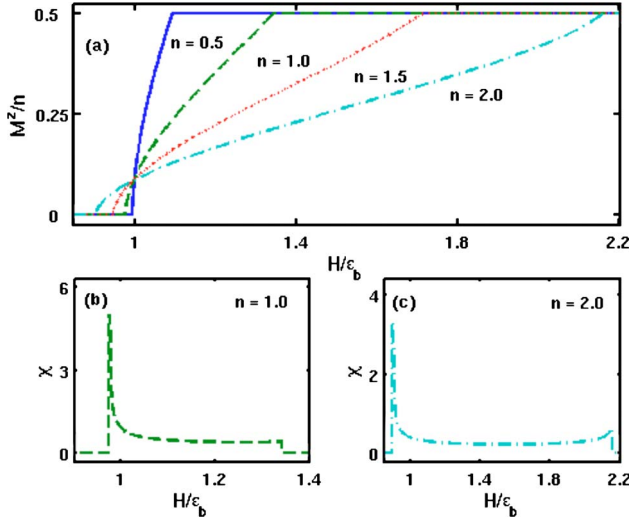


FIG. 2. (Color online) Magnetization M^z and susceptibility χ vs the external field H in the units $2m=\hbar=1$, according to Eq. (39).

proach the binding energy ϵ_b . The two critical fields have opposite monotonicity: H_{c1} decreases with increasing n whereas H_{c2} increases with n . For the 1D Fermi gas in a harmonic trapping potential,^{21,22} the density is position dependent and decreases away from the trapping center. Thus, for sufficiently large center density, the system has subtle segments; the mixed phase lies in the center and the fully paired phase (or the fully unpaired phase) sits in the two outer wings for $H < \epsilon_b$ (or $H > \epsilon_b$). Nevertheless, for sufficiently low center density, the cloud is either a fully paired phase or a fully unpaired phase for $H < \epsilon_b$, or $H > \epsilon_b$, respectively.

For the 1D Fermi gas, the local pair correlation is defined by

$$g_p^{(1)} = \langle \phi_{\uparrow}^{\dagger}(0) \phi_{\uparrow}^{\dagger}(0) \phi_{\uparrow}(0) \phi_{\uparrow}(0) \rangle \approx \frac{1}{2} \frac{dE}{dc}. \quad (41)$$

For weakly attractive interaction,

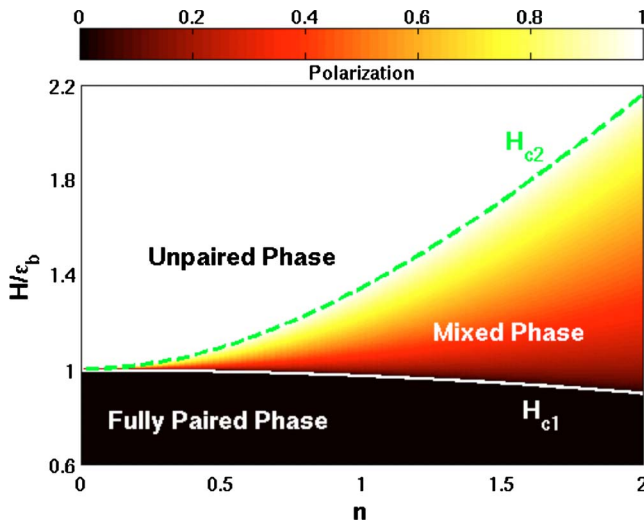


FIG. 3. (Color online) Phase diagram for homogeneous systems with $|c|=10$ according to Eqs. (33), (36), and (39).

$$g_p^{(1)} \approx n^2(1-P^2)/4, \quad (42)$$

indicating a two-component free Fermi gas phase. For strongly attractive interaction, the local pair correlation is given by

$$\frac{g_p^{(1)}}{n^2} \approx \frac{(1-P)}{4} \left[|\gamma| + \frac{\pi^2(1-P)^2(1+3P)}{24\gamma^2} + \frac{8\pi^2P^3}{3\gamma^2} \right]. \quad (43)$$

This has maximum and minimum values corresponding to the fully paired phase for $H < H_{c1}$ and the fully unpaired phase for $H > H_{c2}$, respectively. Depairing weakens the pair correlation in the region $H_{c1} < H < H_{c2}$. The phase transitions in the vicinities of the critical points are of second order.

V. EXCLUSION STATISTICS

Strong thermal fluctuations can destroy the magnetically ordered phases, delineated by the two critical fields, above a critical temperature T_c , which, in principle, can be also calculated from the TBA equations. On the other hand, at temperatures much lower than the degeneracy temperature $T_d := \frac{\hbar^2}{2m} n^2 \ll \epsilon_b$, the bound pairs are stable against weak thermal fluctuations. However, the individual pair wave functions do not overlap coherently, i.e., the existence of bound pairs does not lead to long range order at finite temperatures. This can be seen from the finite temperature TBA equations [Eq. (14)] in which the unpaired band is empty due to a large negative chemical potential. This behavior is similar to that of three-dimensional (3D) attractive fermions.³² In 1D, the dynamical interaction and the statistical interaction in the pairing scattering process are inextricably related.^{33–36} This means that one bound pair excitation may cause a fractional number of holes below the Fermi surface due to the collective signature. This is the key point in understanding GES for 1D interacting many-body systems. We shall show that the bound pairs can be viewed as ideal particles obeying GES. GES has recently been applied to the 3D unitary Fermi gas.³⁷

In the absence of the magnetic field and at low temperatures, the unpaired dressed energy is positive due to a large negative chemical potential. It follows that the BA and TBA equations can be written as

$$\sigma(k) + \sigma^h(k) = \frac{1}{\pi} - \int_{-\infty}^{\infty} a_2(k-\Lambda) \sigma(\Lambda) d\Lambda, \quad (44)$$

$$\epsilon^b(k) = 2 \left(k^2 - \mu - \frac{1}{4} c^2 \right) + Ta_2 * \ln[1 + e^{-\epsilon(k)/k_B T}]. \quad (45)$$

After neglecting exponentially small terms in Eq. (15), the pressure for the bound pairs is given by

$$p^b \approx \frac{2}{\sqrt{2\pi^2 \hbar^2}} \int_0^{\infty} \frac{\sqrt{\epsilon} \epsilon}{1 + e^{[\epsilon - 2A(T)]/k_B T}}, \quad (46)$$

with the function $A(T) := \hbar^2 B^2 / (2m) = (\mu + \frac{1}{4} c^2 - p^b / |2c|)$. Furthermore, using the Sommerfeld expansion and iterating the

pressure p^b with Eq. (45), we obtain the cut-off energy $A(\tau)$ in the form

$$A(\tau) \approx A_0 \left[1 + \frac{16\tau^2}{3\pi^2} \left(1 - \frac{2}{|\gamma|} \right) + \frac{1024\tau^4}{9\pi^4} \left(1 - \frac{4}{|\gamma|} \right) \right], \quad (47)$$

where

$$A_0 = \frac{\hbar^2 n^2 \pi^2}{2m} \left(1 + \frac{1}{|\gamma|} \right). \quad (48)$$

Here, $\tau = K_B T / T_d$ is the degenerate temperature. The pair distribution function $n(\epsilon) := \pi \sigma(\epsilon)$ is given by

$$n(\epsilon) = \frac{1}{\alpha \{ 1 - e^{[\epsilon - 2A(k)] / K_B T} \}}, \quad (49)$$

where $\alpha = 1 + 1/2|\gamma|$.

The chemical potential follows as

$$\mu \approx \mu_0 \left[1 + \frac{16\tau^2}{3\pi^2} \left(1 - \frac{4}{3|\gamma|} \right) + \frac{1024\tau^4}{9\pi^4} \left(1 - \frac{56}{15|\gamma|} \right) \right] - \frac{1}{2} \epsilon_B. \quad (50)$$

Here,

$$\mu_0 \approx \frac{\hbar^2 n^2 \pi^2}{2m} \left(1 + \frac{4}{3|\gamma|} \right), \quad (51)$$

which is consistent with Eq. (29). The total energy per unit length and the free energy per unit length in the strong coupling regime are

$$E \approx E_0 \left[1 + \frac{16\tau^2}{\pi^2} \left(1 - \frac{2}{|\gamma|} \right) + \frac{1024\tau^4}{5\pi^4} \left(1 - \frac{4}{|\gamma|} \right) \right] - \frac{1}{2} n \epsilon_b, \quad (52)$$

$$F \approx E_0 \left[1 - \frac{16\tau^2}{\pi^2} \left(1 - \frac{2}{|\gamma|} \right) - \frac{1024\tau^4}{15\pi^4} \left(1 - \frac{4}{|\gamma|} \right) \right] - \frac{1}{2} n \epsilon_b,$$

respectively. Here,

$$E_0 = \frac{\hbar^2 n^3 \pi^2}{2m} \left(1 + \frac{1}{|\gamma|} \right) \quad (53)$$

is consistent with Eq. (23), obtained from Eq. (16).

We see that in the strongly attractive regime and in the absence of the magnetic field, the bound pairs behave like hard-core bosons at low temperatures and have massless excitations, i.e.,

$$F(T) = F(0) - \frac{\pi C (K_B T)^2}{6 \hbar v_c} + O(T^4). \quad (54)$$

Here, the central charge $C=1$ and v_c is given by Eq. (25). The specific heat is given by

$$c_v = \frac{n K_B \tau}{3 \left(1 + \frac{1}{|\gamma|} \right)} \left[1 + \frac{128\tau^2}{5\pi^2} \left(1 - \frac{2}{|\gamma|} \right) \right]. \quad (55)$$

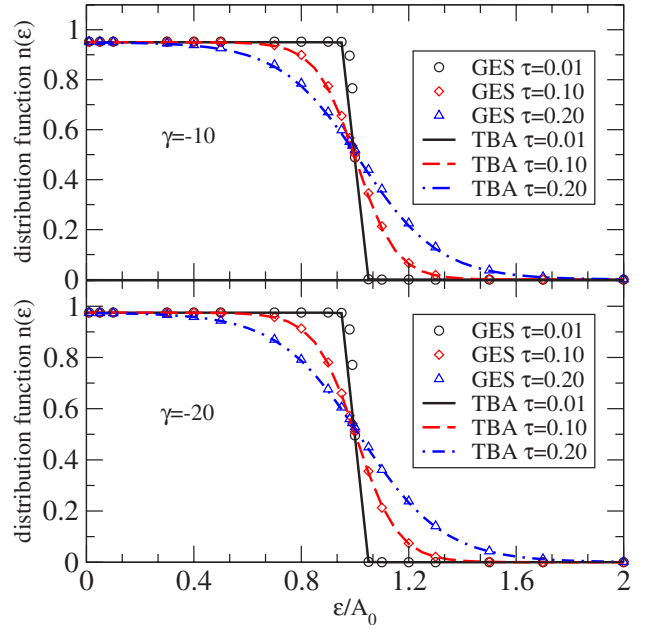


FIG. 4. (Color online) Comparison between the most probable distribution profiles $n(\epsilon)$ for the values $\gamma = -10$ and -20 at different values of the degeneracy temperature $\tau = K_B T / T_d$. At zero temperature, $n(\epsilon) = 1/\alpha$ leads to a Fermi surface at $\epsilon = 2A_0$. Fermi-Dirac statistics with GES parameter $\alpha = 1$ appear for $\gamma \rightarrow \infty$. Attractive interaction thus results in a more exclusive state than for pure Fermi-Dirac statistics. The solid and dashed lines are obtained from the TBA distribution function [Eq. (49)]. The symbols show the most probable distribution evaluated from the GES result [Eq. (56)]. The results from both approaches are seen to coincide well.

On the other hand, the statistical signature of the fully paired state can be described by GES.^{33,35} In this formalism, the pair distribution function is given by

$$n(\epsilon) \approx [(\alpha + w(\epsilon))^{-1}], \quad (56)$$

where $w(\epsilon)$ satisfies the GES relation

$$w^\alpha(\epsilon) [1 + w(\epsilon)]^{1-\alpha} = e^{[\epsilon - 2A(T)] / K_B T}. \quad (57)$$

Here, ϵ denotes the energy of pairs. For the strongly attractive Fermi gas, we find the GES parameter

$$\alpha \approx 1 + 1/2|\gamma|. \quad (58)$$

Now, following Isakov *et al.*,³⁸ at low temperatures, i.e., for $K_B T < T_d$, we find the cut-off energy

$$A(T) \approx A_0 \left[1 + \frac{16\tau^2}{3\pi^2 \alpha^3} + O(\tau^4) \right],$$

which agrees with Eq. (47) to leading order and next leading order in the strong coupling regime (for higher order terms, the reader is referred to Ref. 36). Figure 4 shows the close agreement between the TBA distribution function [Eq. (49)] and the GES's most probable distribution of fermion pairs [Eq. (56)] for different values of interacting strength at low temperatures. We see clearly that the dynamical interaction γ continuously varies the GES, with the most probable distribution of fermion pairs approaching that of hard-core

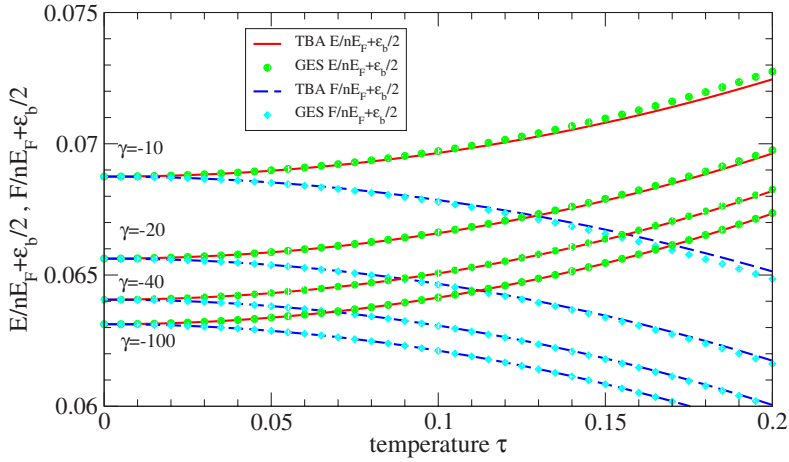


FIG. 5. (Color online) Free energy per unit length $F + \epsilon_b/2$ and total energy per unit length $E + \epsilon_b/2$ in units of $nE_F = \frac{\hbar^2}{2m} \pi^2 n^3/3$ vs the degenerate temperature $\tau = K_B T/T_d$ for different coupling strengths $\gamma = -10, -20, -40, -100$. The solid and dashed lines are evaluated from the TBA results [Eq. (52)]. The symbols follow from the GES results [Eq. (59)]. For $\gamma = -10$, a small discrepancy between the TBA and GES results is observed due to the approximation condition $\gamma \gg 1$. In the strong coupling regime, the universality [Eq. (54)] of low temperature behavior suggests that strongly attractive fermions can be viewed as ideal particles obeying nonmutual GES with $\alpha \approx 1 + 1/|\gamma|$ for temperatures $K_B T \ll \epsilon_b$.

bosonic molecules with an effective statistics parameter $\alpha = 1$ as the interaction increases. In this sense, the dynamical attractive interaction makes the fermions more exclusive. In the GES formalism, the total energy per unit length and the free energy per unit length follow as

$$E \approx E_0 \left[1 + \frac{16\tau^2}{\pi^2 \alpha^3} + O(\tau^4) \right] - \frac{1}{2} n \epsilon_b,$$

$$F \approx E_0 \left[1 - \frac{16\tau^2}{\pi^2 \alpha^3} + O(\tau^4) \right] - \frac{1}{2} n \epsilon_b, \quad (59)$$

which again agree well with the TBA results [Eq. (52)] for strong coupling, see Fig. 5.

VI. CONCLUSION

In conclusion, we have studied pairing and quantum phase transitions in the strongly attractive 1D Fermi gas with an external magneticlike field. Analytic results have been obtained for the critical fields H_{c1} and H_{c2} , magnetization, critical behavior, and local pair correlation. The pairing induced by an interior gap in the system differs from conventional BCS pairing and gapped spin liquids. The smooth pair breaking phase transitions seen in the attractive Fermi gas are reminiscent of the superconductivity breaking phase transitions in type II superconductors.¹³ At low temperatures, we predict that the hard-core bound pairs of fermionic atoms obey GES. The thermodynamics of the hard-core pairs obey universal temperature-dependent scaling.

We emphasize here that in the presence of an external magnetic field, pair breaking in the 1D two-component strongly attractive Fermi gas sheds light in understanding the pairing signature of the 3D strongly interacting Fermi gas of ultracold atoms in which superfluid and normal phases can coexist. Although there is no long range order in 1D quantum many-body physics, the mismatched Fermi surfaces do not prevent pairing. This pairing signature has also been observed in the 3D two-component atomic gas with high spin population imbalances.⁸ In addition, for the 1D Fermi gas, the magnetic field triggers spin imbalances when the external field is greater than the first critical field H_{c1} [Eq. (33)] and less than the second critical field H_{c2} [Eq. (36)]. The energy transfer relation [Eq. (40)] found for this model is also consistent with experimental observations in the 1D Fermi gas.²³ The phase diagram presented in Fig. 3 clearly shows the phase separation and the pairing signature with changing magnetic field. It may be possible to experimentally test our theoretical predictions for the quantum phase transitions and critical fields in the 1D two-component strongly interacting Fermi gas via experimental advances in trapping ultracold atoms.

ACKNOWLEDGMENTS

This work has been supported by the Australian and German Research Councils. The authors thank M. Takahashi for helpful discussions and C.L. thanks Yu. S. Kivshar for support.

¹M. Lewenstein, A. Sanpera, V. Ahufinger, B. Damski, A. Sen, and U. Sen, *Adv. Phys.* **56**, 243 (2007).

²R. Grimm, arXiv:cond-mat/0703091.

³A. Imambekov, V. Gritsev, and E. Demler, arXiv:cond-mat/0703766.

⁴M. W. Zwierlein, A. Schirotzek, C. H. Schunck, and W. Ketterle, *Science* **311**, 492 (2006); M. W. Zwierlein, C. H. Schunck, A. Schirotzek, and W. Ketterle, *Nature (London)* **442**, 54 (2006); Y.

Shin, M. W. Zwierlein, C. H. Schunck, A. Schirotzek, and W. Ketterle, *Phys. Rev. Lett.* **97**, 030401 (2006).

⁵G. B. Partridge, W. H. Li, R. I. Kamar, and R. G. Hulet, *Science* **311**, 503 (2006); G. B. Partridge, W. H. Li, Y. H. Liao, R. G. Hulet, M. Haque, and H. T. C. Stoof, *Phys. Rev. Lett.* **97**, 190407 (2006).

⁶G. Sarma, *J. Phys. Chem. Solids* **24**, 1029 (1963).

⁷P. Fulde and R. A. Ferrell, *Phys. Rev.* **135**, A550 (1964); A. I.

- Larkin and Yu. N. Ovchinnikov, *Sov. Phys. JETP* **20**, 762 (1965).
- ⁸C. H. Schunck, M. W. Zwierlein, A. Schirotzek, and W. Ketterle, arXiv:cond-mat/0702066.
- ⁹W. V. Liu and F. Wilczek, *Phys. Rev. Lett.* **90**, 047002 (2003).
- ¹⁰Michael McNeil Forbes, E. Gubankova, W. V. Liu, and F. Wilczek, *Phys. Rev. Lett.* **94**, 017001 (2005).
- ¹¹M. A. Cazalilla, A. F. Ho, and T. Giamarchi, *Phys. Rev. Lett.* **95**, 226402 (2006).
- ¹²J. Dukelsky, G. Ortiz, S. M. A. Rombouts, and K. Van Houcke, *Phys. Rev. Lett.* **96**, 180404 (2006).
- ¹³B. B. Goodman, *Rev. Mod. Phys.* **36**, 12 (1964); T. G. Berlincourt, *ibid.* **36**, 19 (1964).
- ¹⁴M. Alford, K. Rajagopal, and F. Wilczek, *Phys. Lett. B* **422**, 247 (1998); *Nucl. Phys. B* **537**, 443 (1999).
- ¹⁵A. Rapp, G. Zaránd, C. Honerkamp, and W. Hofstetter, *Phys. Rev. Lett.* **98**, 160405 (2007).
- ¹⁶C. N. Yang, *Phys. Rev. Lett.* **19**, 1312 (1967).
- ¹⁷M. Gaudin, *Phys. Lett.* **24**, 55 (1967).
- ¹⁸M. Takahashi, *Thermodynamics of One-Dimensional Solvable Models* (Cambridge University Press, Cambridge, 1999).
- ¹⁹J. N. Fuchs, A. Recati, and W. Zwerger, *Phys. Rev. Lett.* **93**, 090408 (2004); I. V. Tokatly, *ibid.* **93**, 090405 (2004); G. E. Astrakharchik, D. Blume, S. Giorgini, and L. P. Pitaevskii, *ibid.* **93**, 050402 (2004).
- ²⁰T. Iida and M. Wadati, *J. Phys. Soc. Jpn.* **74**, 1724 (2005).
- ²¹G. Orso, *Phys. Rev. Lett.* **98**, 070402 (2007).
- ²²H. Hu, X.-J. Liu, and P. D. Drummond, *Phys. Rev. Lett.* **98**, 070403 (2007).
- ²³H. Moritz, T. Stoferle, K. Guenter, M. Kohl, and T. Esslinger, *Phys. Rev. Lett.* **94**, 210401 (2005).
- ²⁴M. T. Batchelor, *Phys. Today* **60**(1), 36 (2007).
- ²⁵C. N. Yang and C. P. Yang, *J. Math. Phys.* **10**, 1115 (1969).
- ²⁶A. M. Tsvelick and P. B. Wiegmann, *Adv. Phys.* **32**, 453 (1983).
- ²⁷P. Schlottmann, *Int. J. Mod. Phys. B* **11**, 355 (1997).
- ²⁸F. H. L. Essler, H. Frahm, F. Göhmann, A. Klümper, and V. E. Korepin, *The One-Dimensional Hubbard Model* (Cambridge University Press, Cambridge, 2005).
- ²⁹M. T. Batchelor, X. W. Guan, N. Oelkers, and Z. Tsuboi, *Adv. Phys.* **56**, 465 (2007).
- ³⁰M. T. Batchelor, M. Bortz, X. W. Guan, and N. Oelkers, *J. Phys.: Conf. Ser.* **42**, 5 (2006); N. Oelkers, M. T. Batchelor, M. Bortz, and X. W. Guan, *J. Phys. A* **39**, 1073 (2006).
- ³¹K. Yang, *Phys. Rev. B* **63**, 140511(R) (2001).
- ³²C. Chin, M. Bartenstein, A. Altmeyer, S. Riedl, S. Jochim, J. H. Denschlag, and R. Grimm, *Science* **305**, 1128 (2004).
- ³³Y.-S. Wu, *Phys. Rev. Lett.* **73**, 922 (1994); D. Bernard and Y.-S. Wu, arXiv:cond-mat/9404025.
- ³⁴C. Nayak and F. Wilczek, *Phys. Rev. Lett.* **73**, 2740 (1994).
- ³⁵F. D. M. Haldane, *Phys. Rev. Lett.* **67**, 937 (1991).
- ³⁶M. T. Batchelor, X.-W. Guan, and N. Oelkers, *Phys. Rev. Lett.* **96**, 210402 (2006); M. T. Batchelor and X.-W. Guan, *Phys. Rev. B* **74**, 195121 (2006).
- ³⁷R. K. Bhaduri, M. V. N. Murthy, and M. K. Srivastava, arXiv:cond-mat/0606117.
- ³⁸S. B. Isakov, D. P. Arovas, J. Myrheim, and A. P. Polychronakos, *Phys. Lett. A* **212**, 299 (1996).